Sensitive imaging of an elastic nonlinear wave-scattering source in a solid

Vyacheslav V. Kazakov
Hydroacoustics Laboratory, Institute of Applied Physics, Nizhny Novgorod 603600, Russia

Alexander Sutin
Davidson Laboratory, Stevens Institute of Technology, Hoboken, New Jersey 07030

Paul A. Johnson[a)]
Geophysics, Los Alamos National Laboratory, Los Alamos, New Mexico 87545

(Received 18 February 2002; accepted for publication 24 May 2002)

We have developed an imaging method for locating isolated nonlinear scattering source(s) in solids. It relies on extracting the nonlinear response of a solid by modulation of a high by a low-frequency wave, and employing moving-window, synchronous detection. The resulting image consists of nonlinear wave reflection profiles with remarkable sensitivity to an isolated elastic nonlinear source(s). In creating the image, we can distinguish between a nonlinear scattering source and other wave scatterers in the material. The method should work equally well for imaging the relative nonlinearity of different regions within a volume. © *2002 American Institute of Physics.* [DOI: 10.1063/1.1495081]

In this work we illustrate a method by which to create an image, a ''nonlinear wave reflection profile,'' much like a pulse-echo profile, but one that ''filters'' for nonlinear elastic scattering sources due to material damage. A line scattering source (a crack) is imaged in a sample in the presence of other features that scatter the elastic wave field.

It has been shown that ''low-aspect-ratio'' (flat) features (cracks, grain contacts, delaminations) create ''nonclassical'' nonlinear wave effects while other geometries (spheres, holes, ellipses, surfaces) do not.[1] Nonclassical nonlinearity arises from hysteresis in the wave pressure-deformation (stress-strain) relation,[1] in contrast to ''classical'' (landau-type) nonlinearity arising from anharmonicity.[2]

Work relating material damage and nonlinear dynamic wave response by study of the wave second harmonic was performed as early as 1979,[3] and later,[4] including development of a 2nd harmonic A-scan.[5] Synchronous detection of cracks using modulation has been referred to in a number of works.[6,7]

In the work presented here, synchronous, phase lock detection is combined with nonlinear wave modulation for imaging nonlinear scattering sources. A low-frequency, continuous wave (cw) excitation is applied to the specimen simultaneous to a group of high frequency tone bursts. Due to the cw excitation, the amplitude and phase of the ultrasonic toneburst reflected from a nonlinear source will be modulated, while the signal reflected from an elastically ''linear'' scatterer (e.g., a hole or a material boundary) creates no modulation (see also Ref. 6). One can see the difference schematically in Fig. 1. The figure shows tone bursts reflected from a linear and nonlinear scatterer, respectively, at different times in the presence of the cw-induced stress field. The amplitude of the wave reflected from the nonlinear scatterer is controlled by the phase of the cw excitation. The first pair of tone bursts is reflected at a point when the low-frequency cw excitation stress reaches a maximum, forcing a transient, reduced acoustic impedance. The second pair of tone bursts is shown at the time when the low-frequency wave stress is zero, meaning there is no effect on the reflected tone bursts. The third pair is shown at the moment of wave extension, forcing a transient reflection coefficient that is maximized. The amplitude of the tone burst reflected from the linear scatterer remains constant, remaining independent of the changing stress field. Application of the amplitude modulation of the ultrasonic tone burst with synchronous detection allows one to distinguish nonlinear from linear scatterers.

In the following we provide specific details about the procedure. In Fig. 2(a) we show a sample with nonscattering sources (small dots), a nonlinear scattering source (bold line at A) and a linear scattering source (large dot at B). Figure 2(b) illustrates the modulation and synchronous detection scheme for isolating the nonlinear scatterer described below.

Three times and rates are pertinent: (1) the two-way travel time associated with each scattering location τ_m, (2) the repetition rate between each high-frequency tone burst R, and (3) the time (duration) of the processed signal T_n at the scattering source location τ_m. In Fig. 2(a) the wave source located on the sample face launches a tone burst (in this experiment the frequency and duration are 3 MHz and 0.66 μs, respectively) at a sequence of times, $T_1 \ldots T_N$, $N=512$.

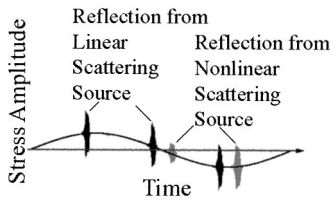

FIG. 1. Concept of the combined effect of low-frequency cw modulation of successive ultrasonic pulses in a material containing a linear and a nonlinear scatterer.

[a)]Author to whom correspondence should be addressed; electronic mail: paj@lanl.gov

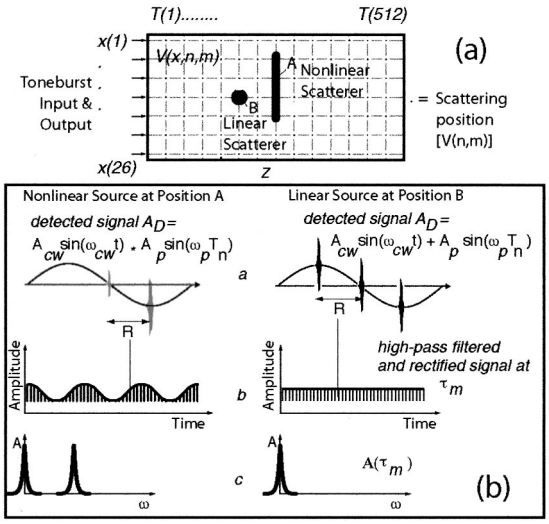

FIG. 2. (a) Conceptual view of the experiment and (b) of the processing scheme.

The vector of radiated pulse sequence T_N is $T_n=(1/R)(n-1)$ s, $n=1...N$, where the source repetition rate R is 366 Hz. Thus at each T_n, we have a tone burst with amplitude A_p from $A_p\sin(\omega_p T_n)$ where the subscript p refers to the tone burst. Simultaneously, a large amplitude, cw low-frequency excitation $A_{\mathrm{cw}}\sin(\omega_{\mathrm{cw}}t)$ is applied to the sample end (see Fig. 3). Here the input sampling rate for the cw wave is much smaller than the repetition rate R that controls the pulsed output. The detected signal $A_D=A_{\mathrm{cw}}\sin(\omega_{\mathrm{cw}}t)+A_p\sin(\omega_p T_n)$ in the case of the linear scatterer or $A_D=A_{\mathrm{cw}}\sin(\omega_{\mathrm{cw}}t)A_p\sin(\omega_p T_n)$ in the case of the nonlinear scatterer in the time interval ΔT, the time window width for each location of interrogation in time [the dots on the grid in Fig. 2(b)]. This step can be seen in (*a*) in Fig. 2(b) for the nonlinear and linear scatter, respectively. In the detected signal A_D the low-frequency excitation is eliminated by a high pass filter, the pulses are rectified [(*b*), Fig. 2(b)], and this signal is recorded and digitized, in this case at 0.6 μs using 256 points (thus $\Delta T=256\times 0.6$ μs). The nonlinear scatterer has a nonzero frequency component at the vibration frequency in addition to a dc component while the linear scatterer has only a dc component.

As a consequence the output is an ''amplitude'' matrix V_{nm} extracted from the sequence of filtered and rectified signals $V_{nm}=V(T_n,\tau_m)$, [(*c*), Fig. 2(b)] where the rectified signal in each successive time window is $\tau_m=m\tau_0$, the sampling interval of the rectified signal $\tau_0=\Delta T/256$, the number of samples in the rectified signal $m=1...256$, and $n=1...N$.

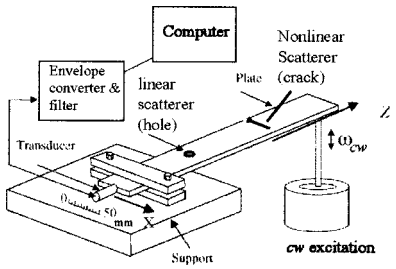

FIG. 3. Experimental configuration.

The basic procedure is to study the Fourier structure of $V(T_n,\tau_m)$ at fixed (phase-locked) τ_m,

$$A(\tau_m)=\sum_{n=1}^{N} V(T_n,\tau_m)\sin\omega_{\mathrm{cw}}T_n, \tag{1}$$

where $V(T_n,\tau_m)$ is at the frequency $\sin\omega_{\mathrm{cw}}T_n$ of the cw modulation, the 10 Hz signal in this case. This procedure will identify those τ_m at which the detected signal has evidence of the nonlinear scatterer, because a nonlinear scatterer will have energy at the modulation-wave frequency and a linear scatterer will not [(*c*), Fig. 2(b)]. The association of time τ_n with space Z_n can be carried out independently of the experimental procedure (if wave speed is known), and therefore the above steps do not depend on this identification. Thus if $\tau\propto Z$ in some known way, the output can be used to identify the spatial location of the nonlinear scatterer. This procedure is carried out for $x_1\ldots x_i$, where $i=1...26$ source locations across the sample face, and in this manner the full wave profile (the two-dimensional matrix of scattered amplitudes) is obtained.

The processed data set is the amplitude of the 10 Hz signal at each x_i and at each τ_m. That is, the X by τ_m matrix of amplitudes is, $A_f(x_i,\tau_m)$, where the subscript f is the modulation frequency at 10 Hz. The location of the scattering source is found by solving the inverse problem associated with this matrix. Here the nonlinear scatterers are point sources to within the resolution $\Delta z=c\tau_0$, where c is wave speed. The amplitude $A_{10\ \mathrm{Hz}}(i,m)$ comes from a source on the line (x_i,z) at $z=mc\tau_0/2\equiv z_m$. We divide by two because we record the two-way travel time of the scattered signals.

The output matrix is similar in form to the absolute value of amplitude in a seismic reflection profile or pulse-echo experiment. A difference with a seismic reflection profile is that we have no off-axis detection in this experiment, although it could and should be done in order to improve nonlinear source resolution and imaging capability.

The experimental configuration is shown in Fig. 3. The sample used to demonstrate the imaging technique was a crack in a steel plate ($50\times 305\times 6$ mm) induced by cyclic loading. Before loading, a notch was placed in the plate surfaces to initiate cracking (located 101.5 mm from the plate ends). The length of the notch was 17 mm, the depth was 0.8 mm, and width was 0.7 mm. A hole 3 mm in diameter was drilled in the plate at a distance of 101.5 mm from the plate end farthest from the crack (see Fig. 3).

One of the plate ends was clamped to a support composed of a large mass. Rubber insertions were placed between the samples, and the clamp and support, to avoid possible nonlinear effects from them. The ultrasonic tone-burst wave was radiated at the plate face as shown in Fig. 3. The diameter of the piston radiator was 9 mm and the resonance frequency of the transducer was 3 MHz. The contact between the transducer and plate was made by a standard lubricant. Triggering was accomplished by using the electrical tone burst applied to the transducer.

The far end of the plate was connected to a mechanical shaker (Robotron 11075). The shaker excited flexural vibration of the plate. Vibration amplitudes were detected and feedback-controlled for amplitude stability by use of an accelerometer located on the plate.

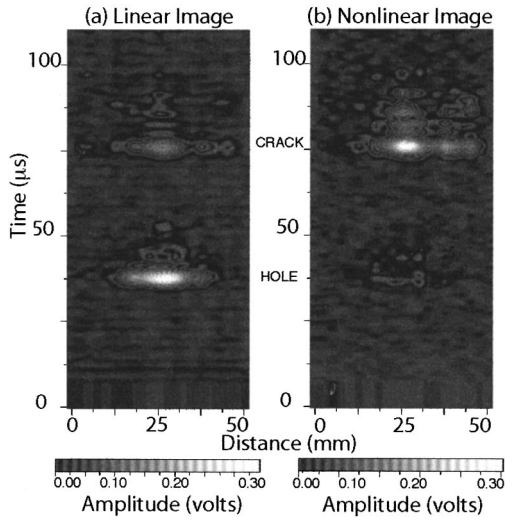

FIG. 4. (a) Elastic linear scatterering profile where the large reflection from the hole is at approximately 35 μs. The crack is the later, smaller reflection. (b) Elastic nonlinear scattering profile where only the crack is imaged. The brighter regions correspond to increased scattering amplitude.

For comparison with a well-known linear method, a pulse-echo experiment was conducted as well. The two dimensional reflection profiles of the elastic linear and of the nonlinear scattering sources $[A_{10\,Hz}(i,m)]$ as a function of time are shown in Figs. 4(a) and 4(b). In Fig. 4(a), it is clear that the amplitude of the linear signal reflected from the hole is higher than amplitude of signal reflected from the crack [Fig. 4(a)]. Both features are imaged, but the nature of the features is unknown without *a priori* knowledge or some other means of testing. In the case of the nonlinear reflection profile the level of the modulation in the signal reflected from crack is large [Fig. 4(b)]. The hole is a linear scatterer and therefore should not produce modulation of the reflected signal. The hole does create some signal for reasons perhaps related to scattering, but nonetheless, the lesson learned from the two reflection profiles is impressive. This experiment clearly demonstrates that a crack can be discriminated within the background of linear scattering from inhomogeneities other than cracks, and including sidewall and backwall reflections.

The spatial resolution of the image depends on the transducer width and the distance to the reflected feature. The radiation angle of the transducer in the plate is given by $\sin\phi = 0.88\lambda/d$ under far field conditions, where ϕ is the ray angle, λ is wavelength, and d is transducer diameter. This expression indicates that the beam width is 19 mm at 100 mm, the distance of the crack. One could narrow the beam width with some effort. Lateral variation in the nonlinear response may well indicate variation in crack parameters, and from the point of view of discerning crack properties, the spatial variation of the nonlinear amplitude may be very important.[1]

This work demonstrates that the tone-burst modulation and synchronous detection technique is an effective tool for selective wave imaging of elastically nonlinear scattering sources in the presence of elastically linear scatterers. Further, the results indicate that the method could be applied to careful study of the spatial distribution of nonlinear scattering properties. Such studies may shed light on such issues as crack initiation, crack progression, and the nagging question of the physical origin of nonclassical, nonlinear behavior (e.g., Ref. 1). Three dimensional imaging is clearly possible applying the same method, and, if multiple offset detectors were used, full, poststack migration imaging could be achieved.

From numerous other studies conducted by us and others, we know that different material volumes of scatterers can display different nonlinear characteristics (e.g., Ref. 1). This method is applicable to the study of mixed volumes where such differences may exist. Conceivable applications include imaging of mixed phase materials, imaging of progressive fatigue, in particular of volumes where the fatigue may not be homogeneous, imaging delaminations in layered composites, and surface seismic and borehole imaging.

The work was supported by the International Science Technical Center and by Los Alamos National Laboratory Institutional Support. Thanks to R. Guyer for helpful discussions.

[1] R. A. Guyer and P. Johnson, Phys. Today **52**, 30 (1999); P. A. Johnson, Mater. World **7**, 544 (1999); K. E. A. Van Den Abeele, P. A. Johnson, and A. M. Sutin, Res. Nondestruct. Eval. **12**, 17 (2000).
[2] L. D. Landau and E. M. Lifschitz, *Theory of Elasticity*, 3rd (revised) English edition (Pergamon, New York, 1986).
[3] O. Buck, W. L. Morris, and J. N. Richardson, Appl. Phys. Lett. **33**, 371 (1978).
[4] O. Rudenko and Chin An Vu, Acoust. Phys. **40**, 593 (1994); D. C. Hurley and C. M. Fortunko, Meas. Sci. Technol. **8**, 634 (1997); P. B. Nagy, Ultrasonics **36**, 375 (1998); M. Rothenfusser, M. Mayr, and J. Baumann, Ultrasonics **38**, 322 (2000); W. Yost, J. Cantrell, and J. K. Na, Rev. Prog. Quant. Nondestr. Eval. **20**, 1268 (2001).
[5] I. Solodov, Ultrasonics **36**, 383 (1998).
[6] H. Xiao and P. Nagy, J. Appl. Phys. **83**, 7453 (1998).
[7] A. S. Korotkov, M. M. Slavinskii, and A. M. Sutin, Acoust. Phys. **40**, 71 (1994); V. E. Nazarov and A. M. Sutin, J. Acoust. Soc. Am. **102**, 3349 (1997); A. E. Ekimov, I. N. Didenkulov, and V. V. Kazakov, J. Acoust. Soc. Am. **106**, 1289 (1999).